

1 **Arabidopsis O-fucosyltransferase SPINDLY regulates root hair patterning independently of** 2 **gibberellin signalling**

3 Krishna Vasant Mutanwad*, Isabella Zangl and Doris Lucyshyn*

4 Institute for Molecular Plant Biology, Department of Applied Genetics and Cell Biology, University of
5 Natural Resources and Life Sciences

6 Muthgasse 18, 1190 Vienna, Austria

7 ORCID IDs: [0000-0003-2856-1953](https://orcid.org/0000-0003-2856-1953) (KVM), [0000-0002-5196-7444](https://orcid.org/0000-0002-5196-7444) (IZ), [0000-0001-8558-1219](https://orcid.org/0000-0001-8558-1219) (DL)

8 *correspondence: doris.lucyshyn@boku.ac.at, krishna.mutanwad@boku.ac.at

9

10

11 **Abstract**

12 Root hairs are able to sense soil composition and play an important role for water and nutrient uptake.
13 In *Arabidopsis thaliana*, root hairs are distributed in the epidermis in a specific pattern, regularly
14 alternating with non-root hair cells in continuous cell files. This patterning is regulated by internal
15 factors such as a number of hormones, as well as external factors like nutrient availability. Thus, root-
16 hair patterning is an excellent model for studying the plasticity of cell fate determination in response
17 to environmental changes. Here, we report that loss-of-function mutants in the Protein O-
18 Fucosyltransferase SPINDLY (SPY) form ectopic root hairs. Using a number of transcriptional reporters,
19 we show that patterning in *spy-22* is affected upstream of the central regulators GLABRA2 (GL2) and
20 WEREWOLF (WER). O-fucosylation of nuclear and cytosolic proteins is an important post-translational
21 modification that is still not very well understood. So far, SPY is best characterized for its role in
22 gibberellin signalling via fucosylation of the growth-repressing DELLA protein REPRESSOR OF GA
23 (RGA). Our data suggest that the formation of ectopic root hairs in *spy-22* is independent of RGA and
24 gibberellin signalling.

25 **Introduction**

26 Post translational modifications (PTM) dynamically modulate various physiological and morphological
27 events throughout the life span of plants (Millar *et al.* 2019). O-Glycosylation of nuclear and cytosolic
28 proteins is one such PTM, and plants carry two O-glycosyltransferases responsible for these
29 modifications: the Protein O-Fucosyltransferase (POFUT) SPINDLY (SPY), and the O-GlcNAc
30 Transferase (OGT) SECRET AGENT (SEC) (Hartweck *et al.* 2002; Olszewski *et al.* 2010; Zentella *et al.*
31 2016; Zentella *et al.* 2017). These proteins regulate significant events in plants, from embryo
32 development to the determination of flowering time and flower development (Hartweck *et al.* 2002;
33 Hartweck *et al.* 2006). *spy* mutants were initially identified due to their resistance to the gibberellin

34 (GA) biosynthesis inhibitor paclobutrazol, leading to constitutively active GA signalling (Jacobsen and
35 Olszewski, 1993; Swain and Olszewski, 1996). Further studies reported that SPY and SEC are involved
36 in GA signalling via modification of the growth repressing DELLA protein RGA (REPRESSOR OF GA)
37 (Silverstone *et al.* 2007; Zentella *et al.* 2016; Zentella *et al.* 2017). *spy* mutants display various
38 phenotypic traits, such as early flowering, early phase transitions, partial male sterility, abnormal
39 trichome formation and disordered phyllotaxy (Silverstone *et al.* 2007). Recently, SEC also was
40 reported to be involved in delaying flowering time in *Arabidopsis* (Xing *et al.* 2018). The majority of
41 the studies thus have focused on the role of O-glycosylation in aerial tissue development and the
42 subsequent phenotypes are often attributed to its participation in GA signalling. SEC and SPY are also
43 active in roots, however their impact on root development and morphogenesis is largely unexplored
44 (Hartweck *et al.* 2006; Silverstone *et al.* 2007; Swain *et al.* 2002).

45 Tissue morphology and cellular organisation are decisive for root development in *Arabidopsis*
46 *thaliana*. Epidermal tissue is comprised of hair-forming trichoblast cells and non-hair-forming
47 atrichoblast cells (Dolan *et al.* 1993; Löffke *et al.* 2015; Scheres and Wolkenfelt, 1998). The
48 arrangement of the hair and non-hair cells is established around the single ring-like layer of cortex
49 cells. A hair cell arises at the junction between and is connected to two cortical cells, while a non-hair
50 cell is usually adhered to only a single cortex cell. Moreover, hair cells are generally separated by non-
51 hair cells between them (Balcerowicz *et al.* 2015; Dolan *et al.* 1994; Salazar-Henao *et al.* 2016). Various
52 transcription factors like GLABRA2 (GL2), WEREWOLF (WER) and CAPRICE (CPC) are responsible for
53 determination of epidermal cell patterning in *Arabidopsis*. GL2 and WER regulate the establishment
54 of non-hair cells (Lee and Schiefelbein, 1999; Masucci *et al.* 1996), whereas CPC activity is required for
55 the formation of hair cells (Wada *et al.* 1997). GL2 expression is promoted by WER via the formation
56 of a multiprotein complex comprised of TRANSPARENT TESTA GLABRA (TTG1), GLABRA3 (GL3) and
57 ENHANCER OF GLABRA3 (EGL3) (Bernhardt *et al.* 2003; Schiefelbein *et al.* 2014). Further, GL2
58 establishes non-hair cell fate by suppressing the expression of root hair-promoting basic Helix-Loop-
59 Helix (bHLH) transcription factors like ROOT HAIR DEFECTIVE 6 (RHD6), RHD6-LIKE1 (RSL1), RSL2, Lj-
60 RHL1-LIKE1 (LRL1), and LRL2 (Balcerowicz *et al.* 2015; Masucci and Schiefelbein, 1996). On the
61 contrary, in root hair cells, expression of WER is strongly reduced. This allows CPC or its paralogs
62 ENHANCER OF TRY AND CPC 1 (ETC1), ETC3 or TRYPTICHON (TRY) to take its place in the
63 TTG1/EGL3/GL3 complex, resulting in negative regulation of GL2 and de-repression of root hair
64 promoting genes, thus establishing root hair cell fate (Lee and Schiefelbein, 2002; Salazar-Henao *et al.*
65 2016).

66 Root hair development is dynamically controlled by environmental factors like reactive oxygen species
67 (ROS) and pH (Monshausen *et al.* 2007). Furthermore, availability of mineral nutrients like inorganic

68 phosphate (Pi) and iron (Fe) in the surroundings also modulates the development and morphology of
69 root hairs (Janes *et al.* 2018; Müller and Schmidt. 2004; Salazar-Henao *et al.* 2016). Similarly,
70 phytohormones like auxin, ethylene and brassinosteroids are known to influence root hair patterning
71 and development (Balcerowicz *et al.* 2015; Borassi *et al.* 2020; Kuppusamy *et al.* 2009; Liu *et al.* 2018;
72 Shibata and Sugimoto, 2019). However, a role of gibberellin (GA) in epidermis morphology, root hair
73 formation and development has not been described as yet, nor a potential role of the O-
74 glycosyltransferases SPY and SEC in this context. *spy* mutants have been previously reported to display
75 an extra layer of cortex cells, the middle cortex (MC), a phenotype associated with high level ROS
76 signalling (Cui *et al.* 2014; Cui and Benfey, 2009). Beyond this, root tissue morphology of *spy* and *sec*
77 mutants is largely unexplored. Hence, we initiated the investigation of the role of SPY and SEC in root
78 development and tissue patterning, also in relation to GA signalling. Here, we show that epidermis
79 morphology and root hair patterning is altered in *spy*, but not in *sec* mutants. Using a set of reporter
80 constructs, we established that SPY regulates patterning upstream of WER. However, we did not find
81 any evidence for an involvement of GA signalling, indicating that SPY regulates root hair patterning
82 independently of DELLA proteins and GA-signalling.

83 **Results**

84 The Arabidopsis Protein O-fucosyltransferase mutant *spy-22* has larger root apical meristems

85 In order to investigate the involvement of O-glycosylation in Arabidopsis root development we
86 analysed various morphological phenotypes of the T-DNA insertion lines *spy-22* and *sec-5* in
87 comparison to wild type Col-0. SPY and SEC regulate GA signalling by modifying the DELLA protein RGA
88 (Silverstone *et al.* 2007; Zentella *et al.* 2016; Zentella *et al.* 2017) and *spy*-mutants display constitutive
89 GA-signalling phenotypes (Jacobsen and Olszewski, 1993). GA deficient mutants like *ga1-3* are
90 reported to have a reduced root apical meristem (RAM) size (Achard *et al.* 2009). To analyse if O-
91 glycosylation is involved in GA-dependent regulation of RAM size, we measured the RAM of 7-day old
92 seedlings, as the region from quiescent centre till the uppermost first cortical cell which is twice as
93 long as wide (Feraru *et al.* 2019). We observed that *spy-22* mutants displayed a significantly longer
94 meristem (347.6 +/- 34.65 μ m) compared to the wildtype Col-0 (283.6 +/- 31.92 μ m) and *sec-5* (282.4
95 +/- 27.51 μ m) (Figure 1 A, B). On counting the number of epidermal cells in the meristem, we found
96 that the number of cells correlated with meristem size, showing a higher number of cells in *spy-22*
97 (39.10 +/- 4.599) compared to Col-0 (29.05 +/- 3.965) and *sec-5* (28.92 +/- 5.008) (Figure S 1). This
98 result is in line with the effect of increased GA-signalling on cell division and meristem size (Achard *et*
99 *al.*, 2009).

100 Additional to cell number, also the patterning and distribution of atrichoblasts (non-hair) and
101 trichoblast (hair) cells of the epidermis is crucial in determining the size of the meristematic region in
102 Arabidopsis (Löfke *et al.* 2013). While analysing our mutants, we observed that the difference between
103 atricho- and trichoblast cell sizes was reduced in *spy-22* mutants compared to wild-type and *sec-5*. To
104 quantify that, we measured the lengths of the last four consecutive cells in adjacent (trichoblast and
105 atrichoblast) cell files in the epidermis marking the transition to the root meristem differentiation zone
106 (Lofke *et al.* 2015). We noted that the atrichoblast cells in Col-0 and *sec-5* (16.21 +/- 4.30 μm and
107 18.05 +/- 3.62 μm respectively) were significantly longer than trichoblast cells (11.70 +/- 2.81 μm and
108 12.38 +/- 2.95 μm respectively). In *spy-22*, atrichoblast cells (15.92 +/- 4.08 μm) were only slightly
109 longer than cells in corresponding trichoblast files (13.49 +/- 4.30 μm) (Figure 1 C, D). This difference
110 was clearly reflected in a lower ratio of atrichoblast/trichoblast cell length in *spy-22* (1.27) compared
111 to Col-0 (1.44) and *sec-5* (1.53) (Figure 1 E). Taken together, we observed both an increase in cell
112 number, as well as an altered distribution of atrichoblast/trichoblast cell length in *spy-22*, resulting in
113 an increase of root meristem size.

114 *spy* mutants display ectopic root hairs

115 The atypical atricho-to trichoblast morphology in *spy-22* led us to explore the consequences of this
116 observation on root hair development in fully differentiated epidermis cells. In *spy-22*, we frequently
117 observed appearance of two trichoblast cell files developing root hairs adjacent to each other,
118 indicating ectopic root hair formation, while in Col-0 and *sec-5* root hair cell files were always
119 separated from each other by a non-hair cell file (Figure 2 A). The underlying cause for the appearance
120 of ectopic root hairs in *spy-22* was further analysed with the help of reporter lines. We used cell type
121 specific promoter-YFP fusions as described (Marquès-Bueno *et al.* 2016) to monitor the expression of
122 transcription factors implicated in root hair patterning at different stages of development. We initially
123 targeted WER which is involved at an early stage of non-hair cell determination and is expressed
124 strongly in atrichoblast cells and weakly in trichoblasts (Lee and Schiefelbein, 1999). On crossing the
125 WER::4xYFP reporter with *spy-22* and *sec-5*, we observed an uneven signal distribution within single
126 cell files in *spy-22* (Figure 2 B). We also crossed our lines to GL2::4xYFP, which in the wild type is
127 exclusively expressed in the atrichoblasts in the cell division and transition zone. While in Col-0 and
128 *sec-5* a regular pattern of reporter gene expression was observed, GL2 expression in *spy-22* was very
129 patchy, potentially underlying the formation of ectopic trichoblasts within non-hair cell files and vice
130 versa (Figure 2 C). We next employed a reporter that is active in differentiated root hair cells, to
131 determine if expression patterns in the meristematic and transition zone match the patterning of
132 developed root hairs in the differentiation zone. EXP7 is expressed specifically in root hair cells. In
133 EXP7::4xYFP *spy-22* we observed non-hair cells without signal within YFP-positive root hair cell files

134 and vice versa, an aberration in reporter expression which we did not detect in the Col-0 or *sec-5*
135 background (Figure 2 D). Taken together, crosses with various transcriptional reporter lines suggest
136 that SPY regulates root hair patterning upstream of WER.

137 It was previously shown that *spy*-mutants generate an additional layer of root cortex cells, which has
138 been attributed to constitutively increased ROS signalling (Cui *et al.* 2014; Cui and Benfey, 2009). This
139 middle cortex between the cortex and the endodermis was also clearly visible in *spy-22* (Figure S2 A).
140 When crossing our lines with SCR::4xYFP to visualize specifically the endodermis, we could confirm
141 the increase in middle cortex formation and clearly distinguish ectopic cell file formation from the
142 endodermis, like seen before (Cui and Benfey, 2009), but there is no indication for a defect in
143 endodermis formation in *spy-22* (Figure S2 B).

144

145 Epidermal cell patterning and ectopic root hair formation in *spy-22* is independent of gibberellin
146 signalling

147 So far, the best-characterised target of SPY is the DELLA protein RGA, which undergoes a
148 conformational change upon O-fucosylation that enhances the interaction with downstream
149 transcription factors, thereby inhibiting their binding to DNA (Zentella *et al.* 2017). As a result, *spy*
150 mutants show constitutively active GA signalling. So far, GA signalling has not been described to play
151 a role in epidermal cell patterning in *Arabidopsis thaliana*, hence we aimed to understand whether
152 the epidermal patterning of *spy-22* was influenced by increased GA signalling. For initial experiments
153 we treated *spy-22*, *sec-5* and Col-0 with 10 μ M GA₃ and measured the tricho- and atrichoblast cell
154 length in the root meristem transition zone. The distribution pattern remained similar to untreated
155 seedlings, as reported in Figure 1 C. The difference in length of trichoblast cells (13.60 +/- 4.21 μ m)
156 and atrichoblast cells (16.15 +/- 3.38 μ m) was smaller in *spy-22* when compared to Col-0 and *sec-5*
157 (Figure 3 A), with a lower atrichoblast/trichoblast ratio (1.3) in *spy-22* also after GA₃ treatment (Figure
158 3 B), at a ratio comparable to the untreated seedlings (compare Figures 1 E and 3 B). Next, we
159 determined GL2::4xYFP expression in Col-0, *spy-22* and *sec-5* upon treatment with 10 μ M GA₃ and
160 analysed the cell file patterning in the cell division and transition zones. We quantified this phenotype
161 by counting the number of patterning defects (which we defined as the appearance of atrichoblast
162 cells in trichoblast cell files and vice versa) per seedling (Figure 3 C). We observed that Col-0 displayed
163 on average 1.47 patterning defects per seedling, with 7/19 seedlings showing no patterning defects.
164 After treatment with 10 μ M GA₃, frequencies of patterning defects did not significantly change, with
165 an average of 2 per seedling (Figure 3 D). Similarly, there was no significant change in patterning
166 defects in GL2::4xYFP *sec-5* in untreated controls (2.7 patterning defects per seedling) compared to

167 10 μ M GA₃-treated seedlings (2.6 patterning defects per seedling) (Figure 3 D). GL2::4xYFP *spy-22*
168 displayed the highest number of patterning defects per seedling (8.1 per seedling) and this did not
169 change significantly upon treatment with 10 μ M GA₃ (7.6 patterning defects per seedling). These
170 results suggest that exogenous application of gibberellin does not influence epidermal patterning in
171 the genotypes analysed.

172 Gibberellin signalling in Arabidopsis is regulated via its ability to mediate the degradation of DELLA
173 proteins, a family of growth inhibitors. The degradation of DELLAs de-represses the DELLA interacting
174 proteins which in turn positively regulate growth (Bao *et al.* 2020; Davière and Achard, 2016) . Most
175 of the available literature on DELLAs is based on work in the *Ler*-background. In order to mimic an
176 environment with reduced GA signalling also in our mutant lines in Col-0 background, we deleted 17
177 amino acids of the DELLA domain of RGA as described by (Dill *et al.* 2001), preventing its recognition
178 by the GA receptor GID. This resulting *RGA:: Δ RGA* construct was transformed into Col-0, rendering
179 the transformants insensitive to GA and thus constitutively repressing the DELLA interacting proteins.
180 The resulting plant lines displayed similar phenotypes like described before in the *Ler* background,
181 including smaller leaf and rosette size, darker leaves, and reduced inflorescence axis length (Figure
182 S3). We then crossed this line into *sec-5* and *spy-22*, in order to test whether reduced GA signalling
183 impacts on ectopic root hair formation. Examination of *RGA:: Δ RGA* Col-0 roots demonstrated that
184 root hair patterning is similar to that of Col-0, showing no discernible ectopic root hair formation.
185 *RGA:: Δ RGA sec-5* and *RGA:: Δ RGA spy-22* root meristems were indistinguishable from their *sec-5* and
186 *spy-22* parents, respectively, with *RGA:: Δ RGA spy-22* still displaying ectopic root hairs (Figure 4 A).

187 Above experiments suggest that epidermal cell patterning defects and ectopic root hair formation in
188 *spy-22* are independent of GA signalling. Further, we measured the cell size of tricho- and atrichoblasts
189 in the transition zone of *RGA:: Δ RGA* Col-0 root meristems (Figure 4 B) and observed that the ratio
190 between the two cell types was unaltered when compared to values obtained in the Col-0 parent
191 background (Figure 4 C, compare with Figure 1 C, D). These findings suggest that epidermal cell
192 patterning and differentiation in wild type roots is independent of GA signalling.

193 **Discussion**

194 Root hairs are essential for the uptake of water and nutrients, as they can sense nutrients in the soil
195 and react by increasing the root surface in a very flexible way. Root hair patterning is therefore
196 regulated by internal as well as environmental factors, allowing for a high degree of plasticity in the
197 developmental program. Thus, many different pathways feed into the regulation of cell fate
198 determination in the epidermis, including a number of hormones such as auxin, ethylene and
199 brassinosteroids (Balcerowicz *et al.* 2015; Borassi *et al.* 2020; Kuppusamy *et al.* 2009; Liu *et al.* 2018;

200 Shibata and Sugimoto, 2019). Root hair patterning in Arabidopsis has been studied extensively and
201 represents a very useful model system for analysis of plasticity in cell fate determination. In recent
202 years, a number of tools have been made available to monitor the establishment of hair- and non-hair
203 cell files in the root apical meristem, including a set of transcriptional reporters labelling specific cell
204 types (Marquès-Bueno *et al.* 2016). Here, we present evidence that O-fucosylation is involved in
205 establishing root hair cell patterning. Using a number of transcriptional reporters, genetics and
206 phenotypical analysis, we show that root hair cell patterning is impaired in the O-fucosyltransferase
207 mutant *spy-22*. Monitoring the expression of WER by using a transcriptional reporter suggests that
208 the patterning defect in *spy-22* is established already early on during epidermal cell fate
209 determination, potentially due to defects in cortex development or cell-to cell communication
210 between cortex and epidermis, as these processes regulate cell type specific WER expression levels.
211 The atypical receptor-like kinase SCRAMBLED (SCR) plays an important role in signalling from the
212 cortex to the epidermis and further on to WER in this context (Gao *et al.* 2019; Kwak *et al.* 2005).
213 Further experiments targeting the function, localization or turn-over of SCR might help determining
214 how SPY participates in cell-to-cell communication at this stage, or alternatively in upstream signalling
215 events in the cortex. Other potential targets of SPY include the transcription factor JACKDAW (JKD),
216 that is expressed in the cortex and regulates epidermal cell fate in a non-cell autonomous way or other
217 regulators of SCR, such as QKY (Hassan *et al.* 2010; Song *et al.* 2019).

218 Post-translational modification by attachment of O-fucose or O-GlcNAc is still not very well
219 understood in plants. The best studied target is the gibberellin signalling repressor RGA, where O-
220 GlcNAc and O-fucose have opposite effects on its activity, probably by inducing conformational
221 changes (Zentella *et al.* 2016; Zentella *et al.* 2017). Accordingly, *spy*-mutants show many phenotypes
222 that can be associated with gibberellin signalling, such as paclobutrazol resistance, early flowering, or
223 elongated growth (Olszewski *et al.* 2010; Silverstone *et al.* 2007). In our study, we did not find an
224 indication that consequences of altered O-fucosylation on root hair-patterning would require
225 gibberellin signalling, as exogenous application of GA did not affect patterning (Figure 3). Consistently,
226 we did not observe root hair patterning defects in *RGA::ΔRGA* lines (Figure 4). The observed increase
227 in cell numbers of *spy-22* meristems (Figure S1) is probably independent of the patterning defect, but
228 further studies are necessary to address if this increased cell division is dependent on GA-signalling.

229 Overall, we suggest a model, where SPY regulates root hair cell fate determination by affecting the
230 spatial order of WER-expression, which then signals down to patchy expression of GL2 and EXP7,
231 leading to ectopic root hair formation (Figure 2). Thus, O-glycosylation potentially regulates the
232 function of upstream regulators such as SCM or the cell-to-cell communication from cortex to the

233 epidermis (Figure 4 D), but further studies are necessary to reveal the direct targets of SPY in this
234 context.

235 **Methods**

236 Plant material and growth conditions

237 All mutant lines used in this study were obtained from the Nottingham Arabidopsis Stock Centre NASC.
238 Col-0 ecotype of *Arabidopsis thaliana* is referred to as wild-type control. T-DNA insertion lines of *spy*-
239 22 (SALK_090582) and *sec-5* (SALK_034290) and previously published reporter lines WER::4xYFP
240 (N2106117), GL2::4xYFP (N2106121) and EXP7::4xYFP (N2106118) (Marquès-Bueno *et al.* 2016) in Col-
241 0 background were used. After surface sterilisation with 70% ethanol, the seeds were plated onto half
242 Murashige and Skoog medium (2.15 g/L MS Salts, 0.25 g/L MES, pH 5.7, 1% agar). After stratification
243 in the dark at 4°C for 2 days, they were vertically grown in long day conditions (16 hours light / 8 hours
244 dark) at 22°C.

245 Microscopy

246 For imaging, a Leica TCS SP5 confocal microscope with an HCX PL APO CS 20.0x0.70 IMM UV objective
247 was used. Seedlings were mounted in Propidium iodide (PI) (0.02 mg/mL) for staining the cell wall
248 prior imaging. DPSS561 Laser was used to excite PI at 561nm (emission 584-735nm with standard
249 PMT), and an Argon Laser at 30 % intensity was used to excite YFP at 514nm (emission 524-552 with
250 HyD detector). Z Stacks were taken for visualizing root hairs and Maximum Projections were made
251 using the Leica LAS AF lite software.

252 Phenotyping and Image quantification

253 Measurements and quantifications were performed using the LAS X Leica Software. For studying the
254 RAM length, seedlings were mounted in PI (0.02 mg/mL). We measured the distance from quiescent
255 centre till the uppermost first cortical cell which was twice as long as wide as described by (Feraru *et*
256 *al.* 2019). For epidermal cell patterning, lengths of 4 consecutive cells from neighbouring
257 (tricho/atrichoblast) files in the late meristem were measured (Lofke *et al.* 2015). For analysing the
258 patterning frequency in GL2::4xYFP, we checked for its expression in cell division and transition zones.
259 We defined the occurrence of trichoblast cells in an atrichoblast cell file and vice versa as a patterning
260 defect and counted the number of such patterning events in each seedling.

261

262 Data Analysis

263 We used GraphPad Prism 5 and 6 for generating graphs. Error bars in graphs indicate standard error.
264 One-way ANOVA and Tukey's Multiple comparison test were performed for statistical analysis of the
265 data. Sample sizes (n) for all experiments are given in the respective figure legends.

266 Plasmid construction and generation of transgenic lines

267 To generate a GA insensitive, stabilized version of RGA in the Col-0 background, *RGA::dRGA* was
268 amplified from genomic DNA of Col-0 using Q5 high fidelity DNA polymerase (NEB). Two overlapping
269 fragments lacking 17 aminoacids covering the DELLA domain like described in (Feng *et al.* 2008) were
270 generated using the following primer pairs: #270 (5'- tacaataaaagcaggctccactagtagtactaattattcgtctgtc-3')
271 and #272 (5'- gttcgagtttcaaagcaacctcgtccatgttacctccaccgtc-3'), #273 (5'-gacggaggaggtaacatggacgaggt
272 tgctttgaaactcgaac-3') and #271 (5'-gctgggtctagatatctcgtgtagcgcgcccgtcagag-3'); The resulting
273 overlapping fragments were then cloned into a Gateway™ pENTR4™ vector backbone linearized with
274 NcoI/XhoI via Gibson Assembly (NEB). The assembled plasmid was transformed into electrocompetent
275 DH10b *E.coli* cells, positive clones were selected on LB medium using kanamycin (50µg/mL) and
276 confirmed by sequencing. Confirmed entry clones were digested with Asil to destroy the kanamycin
277 resistance of the pENTR4-backbone, and recombined with pEarleyGate303 (Earley *et al.* 2006) using
278 Gateway LR Clonase II enzyme mix to generate a plant expression vector. Positive colonies were
279 selected for kanamycin (50µg/mL) resistance, confirmed plasmids were electro-transformed into
280 *Agrobacterium tumefaciens* GV3101 and used for transforming *Arabidopsis thaliana* ecotype Col-0 by
281 floral dipping (Clough and Bent, 1998). Stable transformants with a strong GA-deficient phenotype
282 were selected before crossing with *spy-22* and *sec-5*.

283 Acknowledgements

284 We are grateful to Monika Debreczeny, Barbara Korbei, Jürgen Kleine-Vehn, and members of his group
285 for numerous discussions and support with setting up microscopy techniques, and Mathias Ried for
286 technical support. We thank Christian Luschnig and Melina Velasquez for critically reading the
287 manuscript. Funding was provided by the Austrian Academy of Sciences ÖAW (DOC-fellowship to
288 KVM, APART fellowship to DL) and the Austrian Science Fund FWF (Project number P20051).

289 Author contributions:

290 KVM and DL planned experiments, IZ provided substantial technical support, KVM wrote the
291 manuscript with support by DL.

292

293 References

- 294 **Achard, P. Gusti, A. Cheminant, S. Alioua, M. Dhondt, S. Coppens, F. Beemster, G.T.S. and**
295 **Genschik, P.** (2009) Gibberellin Signaling Controls Cell Proliferation Rate in Arabidopsis. *Current*
296 *Biology*, **19**, 1188–1193.
- 297 **Balcerowicz, D. Schoenaers, S. and Vissenberg, K.** (2015) Cell Fate Determination and the Switch
298 from Diffuse Growth to Planar Polarity in Arabidopsis Root Epidermal Cells. *Frontiers in plant*
299 *science*, **6**, 1163.
- 300 **Bao, S. Hua, C. Shen, L. and Yu, H.** (2020) New insights into gibberellin signaling in regulating
301 flowering in Arabidopsis. *Journal of Integrative Plant Biology*, **62**, 118–131.
- 302 **Bernhardt, C. Lee, M.M. Gonzalez, A. Zhang, F. Lloyd, A. and Schiefelbein, J.** (2003) The bHLH genes
303 GLABRA3 (GL3) and ENHANCER OF GLABRA3 (EGL3) specify epidermal cell fate in the Arabidopsis
304 root. *Development (Cambridge, England)*, **130**, 6431–6439.
- 305 **Borassi, C. Gloazzo Dorosz, J. Ricardi, M.M. Carignani Sardoy, M. Pol Fachin, L. Marzol, E.**
306 **Mangano, S. Rodríguez Garcia, D.R. Martínez Pacheco, J. Rondón Guerrero, Y.D.C. Velasquez,**
307 **S.M. Villavicencio, B. Ciancia, M. Seifert, G. Verli, H. and Estevez, J.M.** (2020) A cell surface
308 arabinogalactan-peptide influences root hair cell fate. *The New phytologist*.
- 309 **Clough, S.J. and Bent, A.F.** (1998) Floral dip: a simplified method for Agrobacterium-mediated
310 transformation of Arabidopsis thaliana. *The Plant journal : for cell and molecular biology*, **16**, 735–
311 743.
- 312 **Cui, H. and Benfey, P.N.** (2009) Interplay between SCARECROW, GA and LIKE HETEROCHROMATIN
313 PROTEIN 1 in ground tissue patterning in the Arabidopsis root. *The Plant journal : for cell and*
314 *molecular biology*, **58**, 1016–1027.
- 315 **Cui, H. Kong, D. Wei, P. Hao, Y. Torii, K.U. Lee, J.S. and Li, J.** (2014) SPINDLY, ERECTA, and its ligand
316 STOMAGEN have a role in redox-mediated cortex proliferation in the Arabidopsis root. *Molecular*
317 *plant*, **7**, 1727–1739.
- 318 **Davière, J.-M. and Achard, P.** (2016) A Pivotal Role of DELLAs in Regulating Multiple Hormone
319 Signals. *Molecular plant*, **9**, 10–20.
- 320 **Dill, A. Jung, H.-S. and Sun, T.-P.** (2001) The DELLA motif is essential for gibberellin-induced
321 degradation of RGA. *PNAS*, **98**, 14162–14167.
- 322 **Dolan, L. Duckett, C.M. Grierson, C. Linstead, P. Schneider, K. Lawson, E. Dean, C. Poethig, R.S. and**
323 **Roberts, K.** (1994) Clonal relationships and cell patterning in the root epidermis of Arabidopsis.
324 *Development*, **120**, 2465–2474.
- 325 **Dolan, L. Janmaat, K. Willemsen, V. Linstead, P. Poethig, R.S. Roberts, K. and Scheres, B.** (1993)
326 Cellular organisation of the Arabidopsis thaliana root. *Development*, **119**, 71–84.
- 327 **Earley, K.W. Haag, J.R. Pontes, O. Opper, K. Juehne, T. Song, K. and Pikaard, C.S.** (2006) Gateway-
328 compatible vectors for plant functional genomics and proteomics. *The Plant journal : for cell and*
329 *molecular biology*, **45**, 616–629.
- 330 **Feng, S. Martinez, C. Gusmaroli, G. Wang, Y. Zhou, J. Wang, F. Chen, L. Yu, L. Iglesias-Pedraz, J.M.**
331 **Kircher, S. Schäfer, E. Fu, X. Fan, L.-M. and Deng, X.W.** (2008) Coordinated regulation of
332 Arabidopsis thaliana development by light and gibberellins. *Nature*, **451**, 475–479.

- 333 **Feraru, E. Feraru, M.I. Barbez, E. Waidmann, S. Sun, L. Gaidora, A. and Kleine-Vehn, J.** (2019) PILS6
334 is a temperature-sensitive regulator of nuclear auxin input and organ growth in *Arabidopsis*
335 *thaliana*. *Proceedings of the National Academy of Sciences of the United States of America*, **116**,
336 3893–3898.
- 337 **Gao, J. Chaudhary, A. Vaddepalli, P. Nagel, M.-K. Isono, E. and Schneitz, K.** (2019) The *Arabidopsis*
338 receptor kinase STRUBBELIG undergoes clathrin-dependent endocytosis. *J Exp Bot*, **70**, 3881–
339 3894.
- 340 **Hartweck, L.M. Genger, R.K. Grey, W.M. and Olszewski, N.E.** (2006) SECRET AGENT and SPINDLY
341 have overlapping roles in the development of *Arabidopsis thaliana* L. Heyn. *Journal of*
342 *experimental botany*, **57**, 865–875.
- 343 **Hartweck, L.M. Scott, C.L. and Olszewski, N.E.** (2002) Two O-linked N-acetylglucosamine transferase
344 genes of *Arabidopsis thaliana* L. Heynh. have overlapping functions necessary for gamete and
345 seed development. *Genetics*, **161**, 1279–1291.
- 346 **Hassan, H. Scheres, B. and Blilou, I.** (2010) JACKDAW controls epidermal patterning in the
347 *Arabidopsis* root meristem through a non-cell-autonomous mechanism. *Development*
348 (*Cambridge, England*), **137**, 1523–1529.
- 349 **Jacobsen, S.E. and Olszewski, N.E.** (1993) Mutations at the SPINDLY locus of *Arabidopsis* alter
350 gibberellin signal transduction. *The Plant cell*, **5**, 887–896.
- 351 **Janes, G. Wangenheim, D. von, Cowling, S. Kerr, I. Band, L. French, A.P. and Bishopp, A.** (2018)
352 Cellular Patterning of *Arabidopsis* Roots Under Low Phosphate Conditions. *Frontiers in plant*
353 *science*, **9**, 735.
- 354 **Kuppusamy, K.T. Chen, A.Y. and Nemhauser, J.L.** (2009) Steroids are required for epidermal cell fate
355 establishment in *Arabidopsis* roots. *Proceedings of the National Academy of Sciences of the*
356 *United States of America*, **106**, 8073–8076.
- 357 **Kwak, S.-H. Shen, R. and Schiefelbein, J.** (2005) Positional signaling mediated by a receptor-like
358 kinase in *Arabidopsis*. *Science (New York, N.Y.)*, **307**, 1111–1113.
- 359 **Lee, M.M. and Schiefelbein, J.** (1999) WEREWOLF, a MYB-Related Protein in *Arabidopsis*, Is a
360 Position-Dependent Regulator of Epidermal Cell Patterning. *Cell*, **99**, 473–483.
- 361 **Lee, M.M. and Schiefelbein, J.** (2002) Cell pattern in the *Arabidopsis* root epidermis determined by
362 lateral inhibition with feedback. *The Plant cell*, **14**, 611–618.
- 363 **Liu, M. Zhang, H. Fang, X. Zhang, Y. and Jin, C.** (2018) Auxin Acts Downstream of Ethylene and Nitric
364 Oxide to Regulate Magnesium Deficiency-Induced Root Hair Development in *Arabidopsis*
365 *thaliana*. *Plant Cell Physiol*, **59**, 1452–1465.
- 366 **Lofke, C. Dunser, K. Scheuring, D. and Kleine-Vehn, J.** (2015) Auxin regulates SNARE-dependent
367 vacuolar morphology restricting cell size. *eLife*, **4**.
- 368 **Löfke, C. Dünser, K. and Kleine-Vehn, J.** (2013) Epidermal patterning genes impose non-cell
369 autonomous cell size determination and have additional roles in root meristem size control.
370 *Journal of Integrative Plant Biology*, **55**, 864–875.

- 371 **Löfke, C. Scheuring, D. Dünser, K. Schöller, M. Luschnig, C. and Kleine-Vehn, J.** (2015) Tricho- and
372 atrichoblast cell files show distinct PIN2 auxin efflux carrier exploitations and are jointly required
373 for defined auxin-dependent root organ growth. *Journal of experimental botany*, **66**, 5103–5112.
- 374 **Marquès-Bueno, M.d.M. Morao, A.K. Cayrel, A. Platre, M.P. Barberon, M. Caillieux, E. Colot, V.**
375 **Jaillais, Y. Roudier, F. and Vert, G.** (2016) A versatile Multisite Gateway-compatible promoter and
376 transgenic line collection for cell type-specific functional genomics in Arabidopsis. *The Plant*
377 *journal : for cell and molecular biology*, **85**, 320–333.
- 378 **Masucci, J.D. Rerie, W.G. Foreman, D.R. Zhang, M. Galway, M.E. Marks, M.D. and Schiefelbein,**
379 **J.W.** (1996) The homeobox gene GLABRA2 is required for position-dependent cell differentiation
380 in the root epidermis of Arabidopsis thaliana. *Development (Cambridge, England)*, **122**, 1253–
381 1260.
- 382 **Masucci, J.D. and Schiefelbein, J.W.** (1996) Hormones act downstream of TTG and GL2 to promote
383 root hair outgrowth during epidermis development in the Arabidopsis root. *The Plant cell*, **8**,
384 1505–1517.
- 385 **Millar, A.H. Heazlewood, J.L. Giglione, C. Holdsworth, M.J. Bachmair, A. and Schulze, W.X.** (2019)
386 The Scope, Functions, and Dynamics of Posttranslational Protein Modifications. *Annual review of*
387 *plant biology*, **70**, 119–151.
- 388 **Monshausen, G.B. Bibikova, T.N. Messerli, M.A. Shi, C. and Gilroy, S.** (2007) Oscillations in
389 extracellular pH and reactive oxygen species modulate tip growth of Arabidopsis root hairs.
390 *Proceedings of the National Academy of Sciences of the United States of America*, **104**, 20996–
391 21001.
- 392 **Müller and Schmidt.** (2004) Environmentally Induced Plasticity of Root Hair Development in
393 Arabidopsis. *Plant physiology*, **134**, 409–419.
- 394 **Olszewski, N.E. West, C.M. Sassi, S.O. and Hartweck, L.M.** (2010) O-GlcNAc protein modification in
395 plants: Evolution and function. *Biochimica et biophysica acta*, **1800**, 49–56.
- 396 **Salazar-Henao, J.E. Vélez-Bermúdez, I.C. and Schmidt, W.** (2016) The regulation and plasticity of
397 root hair patterning and morphogenesis. *Development (Cambridge, England)*, **143**, 1848–1858.
- 398 **Scheres, B. and Wolkenfelt, H.** (1998) The Arabidopsis root as a model to study plant development.
399 *Plant Physiology and Biochemistry*, **36**, 21–32.
- 400 **Schiefelbein, J. Huang, L. and Zheng, X.** (2014) Regulation of epidermal cell fate in Arabidopsis roots:
401 the importance of multiple feedback loops. *Frontiers in plant science*, **5**, 47.
- 402 **Shibata, M. and Sugimoto, K.** (2019) A gene regulatory network for root hair development. *Journal*
403 *of Plant Research*, **132**, 301–309.
- 404 **Silverstone, A.L. Tseng, T.-S. Swain, S.M. Dill, A. Jeong, S.Y. Olszewski, N.E. and Sun, T.-P.** (2007)
405 Functional analysis of SPINDLY in gibberellin signaling in Arabidopsis. *Plant Physiol.* **143**, 987–
406 1000.
- 407 **Song, J.H. Kwak, S.-H. Nam, K.H. Schiefelbein, J. and Lee, M.M.** (2019) QUIRKY regulates root
408 epidermal cell patterning through stabilizing SCRAMBLED to control CAPRICE movement in
409 Arabidopsis. *Nature communications*, **10**, 1744.

- 410 **Swain, S.M. and Olszewski, N.E.** (1996) Genetic Analysis of Gibberellin Signal Transduction. *Plant*
411 *Physiol.* **112**, 11–17.
- 412 **Swain, S.M. Tseng, T.-S. Thornton, T.M. Gopalraj, M. and Olszewski, N.E.** (2002) SPINDLY is a
413 nuclear-localized repressor of gibberellin signal transduction expressed throughout the plant.
414 *Plant physiology*, **129**, 605–615.
- 415 **Wada, T. Tachibana, T. Shimura, Y. and Okada, K.** (1997) Epidermal cell differentiation in
416 Arabidopsis determined by a Myb homolog, CPC. *Science (New York, N.Y.)*, **277**, 1113–1116.
- 417 **Xing, L. Liu, Y. Xu, S. Xiao, J. Wang, B. Deng, H. Lu, Z. Xu, Y. and Chong, K.** (2018) Arabidopsis O-
418 GlcNAc transferase SEC activates histone methyltransferase ATX1 to regulate flowering. *The*
419 *EMBO Journal*, **37**.
- 420 **Zentella, R. Hu, J. Hsieh, W.-P. Matsumoto, P.A. Dawdy, A. Barnhill, B. Oldenhof, H. Hartweck, L.M.**
421 **Maitra, S. Thomas, S.G. Cockrell, S. Boyce, M. Shabanowitz, J. Hunt, D.F. Olszewski, N.E. and**
422 **Sun, T.-P.** (2016) O-GlcNAcylation of master growth repressor DELLA by SECRET AGENT
423 modulates multiple signaling pathways in Arabidopsis. *Genes & development*, **30**, 164–176.
- 424 **Zentella, R. Sui, N. Barnhill, B. Hsieh, W.-P. Hu, J. Shabanowitz, J. Boyce, M. Olszewski, N.E. Zhou,**
425 **P. Hunt, D.F. and Sun, T.-P.** (2017) The Arabidopsis O-fucosyltransferase SPINDLY activates
426 nuclear growth repressor DELLA. *Nature chemical biology*, **13**, 479–485.
- 427

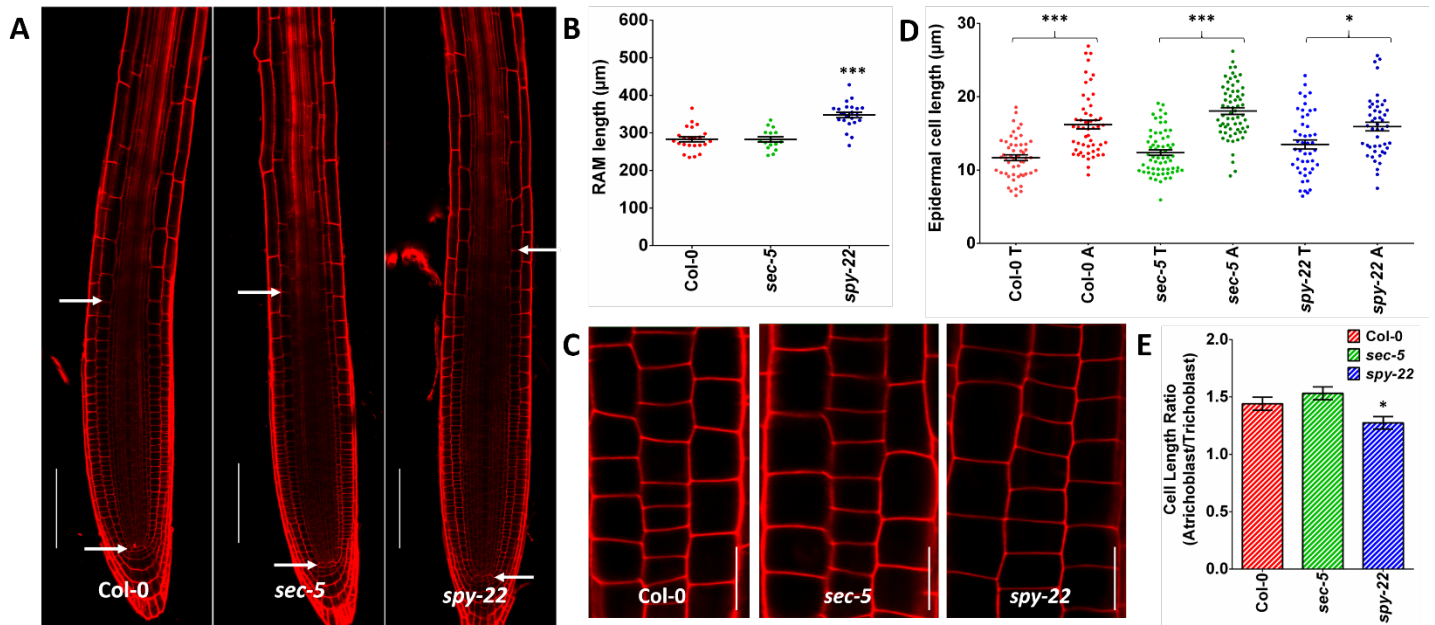


Figure 1. A- Longitudinal cross section images of 7-day old seedlings mounted in PI. Meristem size was defined as the distance from the quiescent center to first uppermost cortical cell which was twice as long as wide, as indicated by white arrows, scale bar – 100µm. B- *spy-22* roots display a significantly longer meristem compared to Col-0 and *sec-5*. n = 16-23. C- The epidermal layer in the late meristematic region of 7-day old seedlings mounted in PI. Lengths of 4 consecutive cells in neighboring (tricho/atrichoblast) files in the late meristem were measured, scale bar – 20µm. D- Atricho- and trichoblast cell length in Col-0, *sec-5* and *spy-22*, n = 47-64. E- The ratio of the epidermal cell lengths of atrichoblasts/trichoblasts is lower in *spy-22* compared to *sec-5* and Col-0. For statistical analysis, One-way ANOVA with Tukey's multiple comparison and students t-test were done (***) $P \leq 0.001$, * $P \leq 0.05$), data from three independent biological repeats is shown.

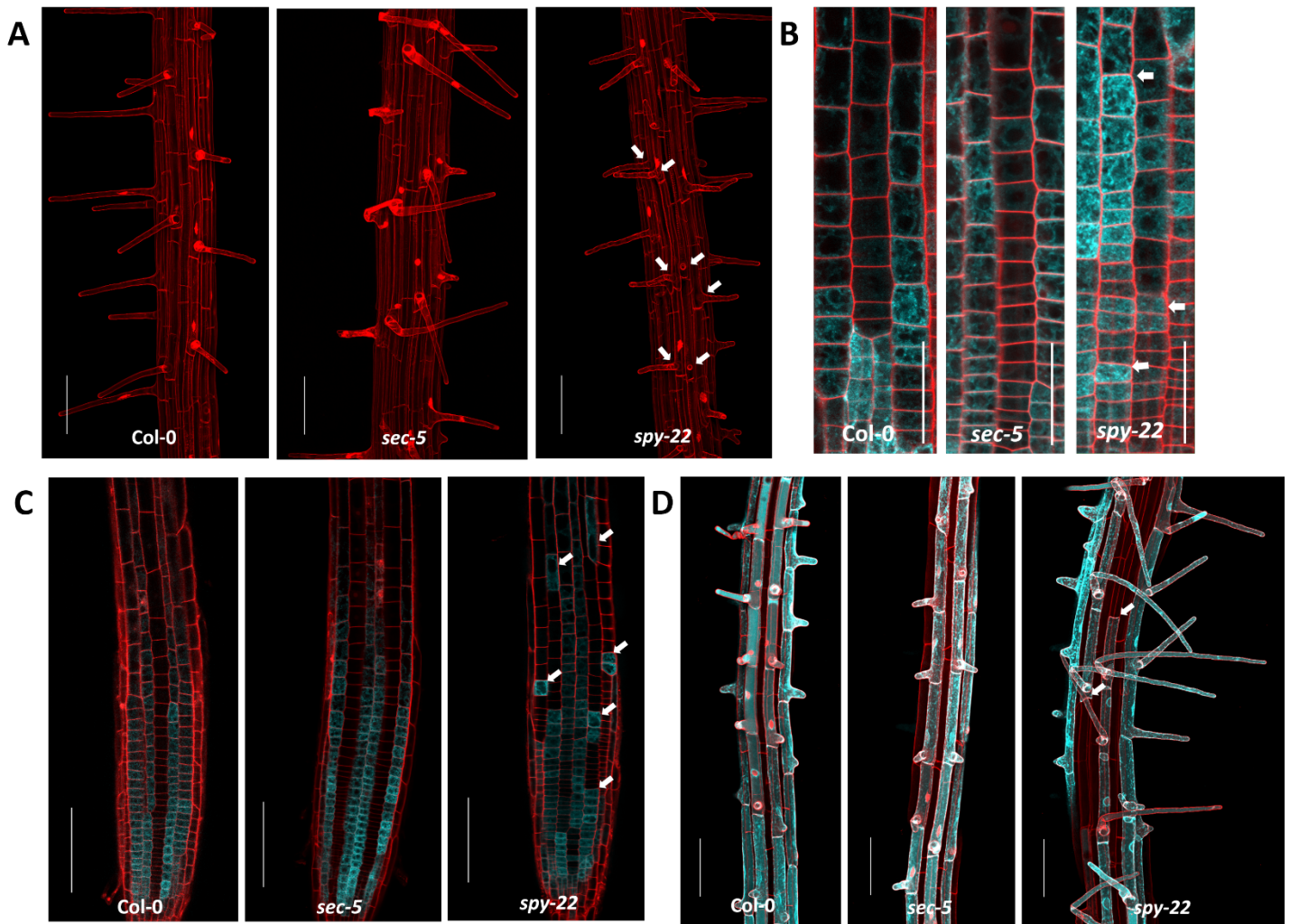


Figure 2. A- Maximum projection of Z stacks to visualize root hair patterning of O-glycosylation mutants. *spy-22* displays ectopic root hairs, scale bar – 100 μ m. B- WER::4xYFP expression in the epidermal cells in the meristem region. YFP signal in *spy-22* is unevenly distributed within the same cell file, scale bar – 50 μ m C- GL2 activity visualized in atrichoblasts expressing GL2::4xYFP. Expression in *spy-22* indicates the presence of trichoblast cells in the atrichoblast cell file and vice versa, scale bar – 100 μ m . D- EXP7 is exclusively expressed in root hair cells. YFP signal indicates EXP7 promoter activity is not uniform within cell files in *spy-22*, suggesting the presence of atrichoblasts in a trichoblast cell file and vice versa, scale bar – 100 μ m. Representative pictures of three biological repeats are shown.

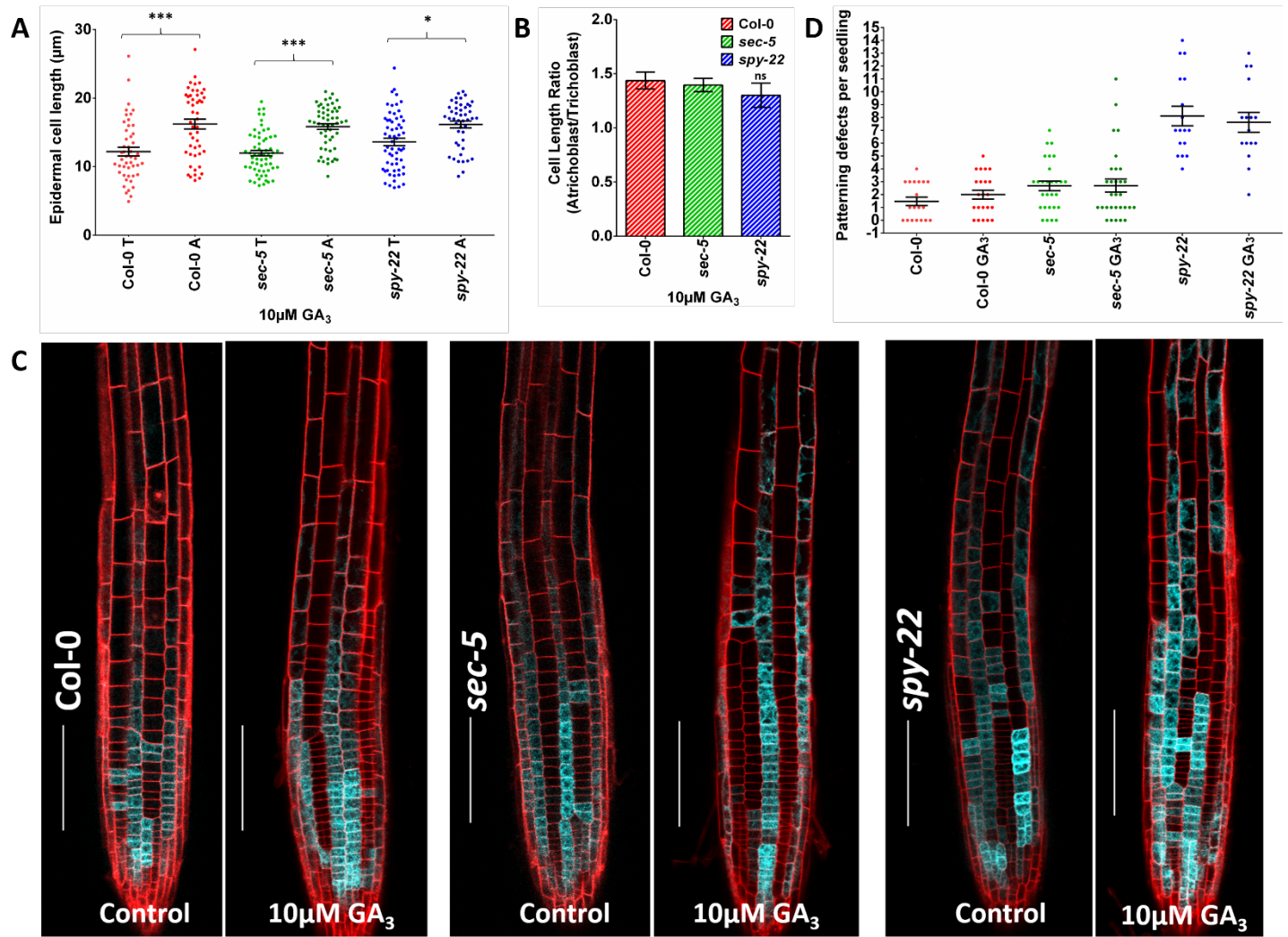


Figure 3. A- Epidermal cell length of 7-day old Col-0, *sec-5* and *spy-22* seedlings grown on $\frac{1}{2}$ MS supplemented with $10\ \mu\text{M}$ GA_3 , $n = 48-60$. B- Presence of $10\ \mu\text{M}$ GA_3 does not influence the epidermal patterning, the ratio of the epidermal cell lengths of atrichoblasts/trichoblasts is lower in *spy-22* compared to *sec-5* and Col-0. C- GL2::4xYFP expression pattern remains largely unchanged in presence of $10\ \mu\text{M}$ GA_3 , scale bar – $100\ \mu\text{m}$. D- Patterning defects per seedling defined as the number of times an atrichoblast appears in trichoblast cell file and vice versa. The average number of patterning events per seedling remained unaffected in the presence of $10\ \mu\text{M}$ GA_3 in all the lines compared to untreated controls. For statistical analysis, One-way ANOVA with Tukey's multiple comparison was done (***) $P \leq 0.001$, * $P \leq 0.05$), data from three biological repeats is shown.

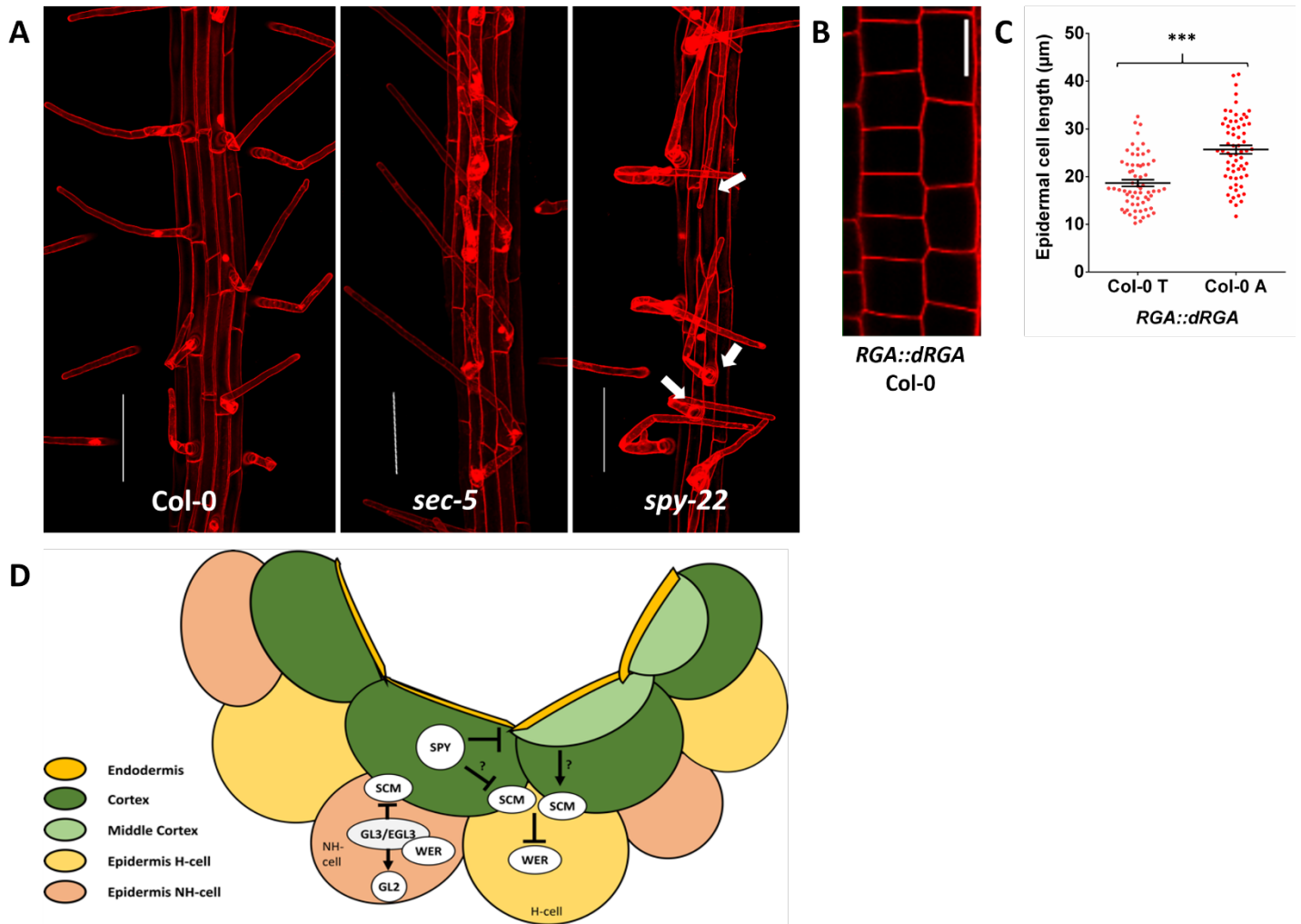
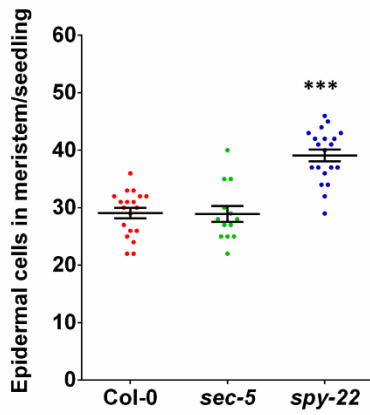
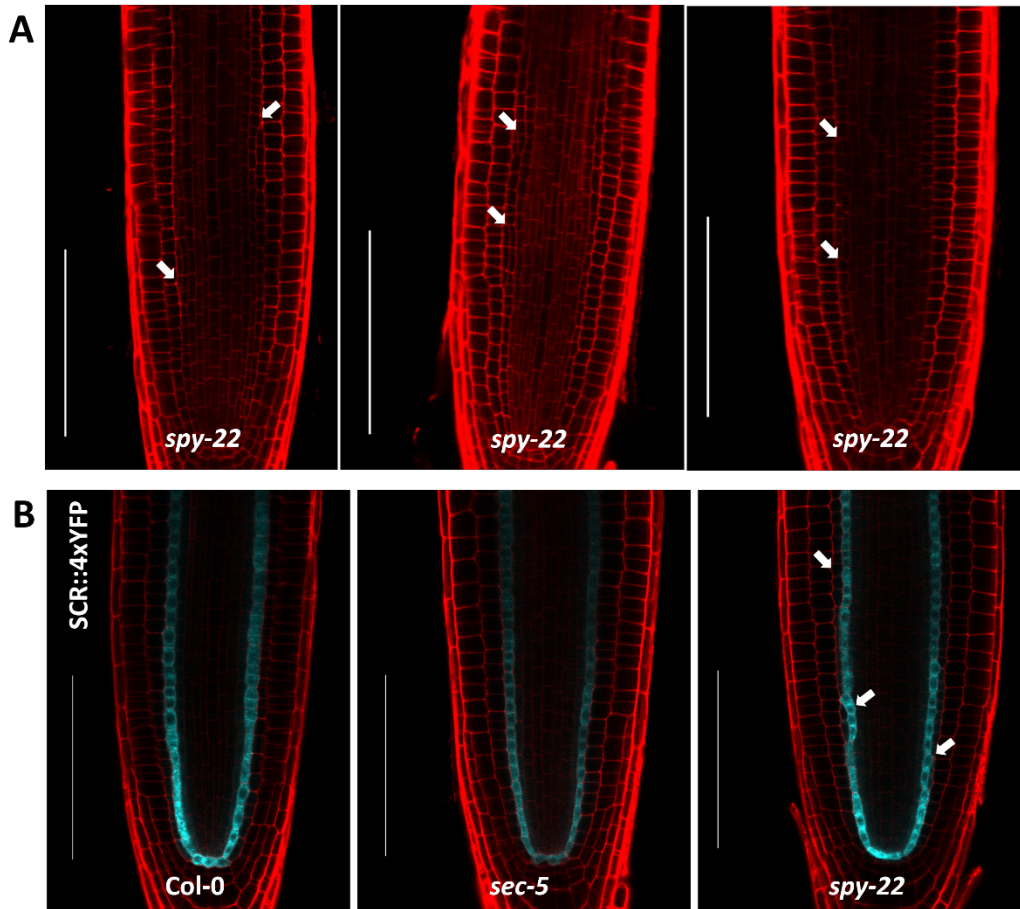


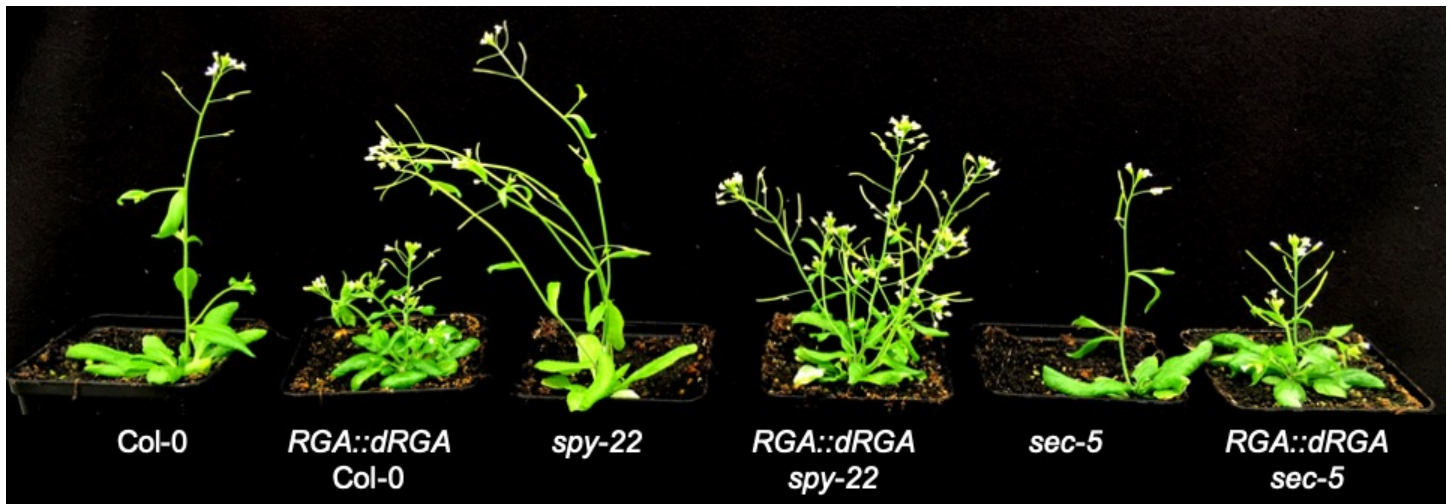
Figure 4. A- 7-day old *RGA::dRGA Col-0*, *RGA::dRGA sec-5* and *RGA::dRGA spy-22* seedlings grown on ½ MS agar mounted in PI. *RGA::dRGA Col-0* and *RGA::dRGA sec-5* did not show ectopic root hairs, while in *RGA::dRGA spy-22* ectopic root hair formation was comparable to *spy-22* (see Figure 2 A), scale bar – 100 μm. B- Epidermal layer of 7 day old *RGA::dRGA Col-0* seedling in the late meristematic region. The length of 4 consecutive cells in neighbouring tricho- and atrichoblast files were measured, scale bar – 20 μm. C- In *RGA::dRGA Col-0*, atrichoblasts cells are significantly larger than trichoblast cells, similar to Figure 1 D and 3 A. For statistical analysis a Students T-test was done (***) P ≤ 0.001). D- Model describing the role of SPY in root hair patterning. H-cell: root hair cell/trichoblast. NH-cell: non-root hair cell/atrichoblast.



Supplement Figure 1 – Number of epidermal cells in the meristem of 7 DAG O-glycosylation mutants. Meristem of *spy-22* mutants have a higher number of epidermal cells (39.10 +/- 4.599) compared to Col-0 (29.05 +/- 3.965) and *sec-5* (28.92 +/- 5.008). For statistical analysis, One-way ANOVA with Tukey's multiple comparison was done (***) P ≤ 0.001), data from three independent biological repeats is shown.



Supplement Figure 2 A – 7-day old *spy-22* seedlings grown on ½ MS agar mounted in PI, arrows indicate middle cortex formation. This extra layer of cortex is formed between cortex and endodermis and has been previously described by Cui *et al.* 2014. scale bar – 100µm. B - SCR::4xYFP expression in Col-0, *sec-5* and *spy-22* is restricted to the endodermis. The middle cortex proliferation in the *spy-22* background is unique and independent of SCR expression in the endodermis.



Supplement Figure 3. Col-0, *spy-22*, *sec-5* and their crosses with *RGA::dRGA* Col-0, a line expressing a stabilized version of the GA-signaling repressing DELLA protein RGA. All *RGA::dRGA* lines show phenotypes characteristic for low GA signaling, like smaller rosette size and shorter inflorescences.